A novel diagnostic technique to detect the failure mode operating states of an air-breathing fuel cell used in fuel cell vehicles

Attuluri Rakada Vijay Babu*

Department of Electrical and Electronics Engineering,
Vignan's Foundation for Science, Technology & Research,
Guntur, AP 522213, India
Email: 202vijay@gmail.com
*Corresponding author

Panthalingal Manoj Kumar

Department of Mechanical Engineering,
PSG Institute of Technology and Applied Research,
Coimbatore, TN 641062, India
Email: manojpanthalingal@gmail.com

Gorantla Srinivasa Rao

Department of Electrical and Electronics Engineering,
Vignan's Foundation for Science, Technology & Research,
Guntur, AP 522213, India
Email: srn.gorantla@gmail.com

Abstract: The world is at a cusp of major transition to fuel cell technology. Water management is of prime importance in air-breathing fuel cells (ABFCs). Inadequate water management leads to the dehydration or flooding which affects the performance of fuel cell. The paper addresses the issues of water management in ABFC by a novel method. Understanding of flooding and dehydration states is presented through experimental investigations. Experiments are conducted at various operating conditions to identify dehydration, normal or flooding states using easily measurable parameters like cell temperature, voltage and current. Preliminarily, by considering iR drop as a distinguishing parameter, dehydration and flooding operating states are distinguished.

Keywords: ABFC; air-breathing fuel cell; water management; dehydration; flooding; iR drop; operating parameters; cell temperature; cell resistance; diagnostic technique; fuel cell vehicles.

Reference to this paper should be made as follows: Babu, A.R.V., Kumar, P.M. and Rao, G.S. (2020) 'A novel diagnostic technique to detect the failure mode operating states of an air-breathing fuel cell used in fuel cell vehicles', *Int. J. Electric and Hybrid Vehicles*, Vol. 12, No. 1, pp.32–43.

Copyright © 2020 Inderscience Enterprises Ltd.

Biographical notes: Attuluri Rakada Vijay Babu completed his graduation in Electrical and Electronics Engineering at the Vignan's Engineering College, Guntur in 2010 and his post graduation in Energy Engineering at PSG College of Technology, Coimbatore in 2012. Currently he is working as an Assistant Professor in Department of Electrical and Electronics Engineering, VFSTR Deemed to be University, Vadlamudi. His research interests include fuel cells, renewable energy systems and electric vehicles. He has published/presented around 50 research papers in national and international Journals and conferences.

Panthalingal Manoj Kumar completed his graduation in Mechanical Engineering at Calicut University in 1999 and his post graduation in Thermal Engineering at National Institute of Technology Calicut in 2002. He completed his PhD on PEM fuel cells at Indian Institute of Technology Madras, Chennai in 2012. Currently he is working as an associate professor in Department of Mechanical Engineering, PSG Institute of Technology and Applied Research. His research interests include fuel cells, energy and thermal engineering. He has published/presented around 40 research papers in national and international Journals and conferences.

Gorantla Srinivasa Rao completed his graduation in Electrical and Electronics Engineering at Acharya Nagarjuna University, Guntur in 1998 and his post graduation in High Voltage Engineering at Anna University, Chennai in 2002. He completed his PhD on hybrid electric vehicles at Jawaharlal Nehru Technological University, Kakinada in 2015. Currently he is working as a professor in Department of Electrical and Electronics Engineering, VFSTR Deemed to be University, Vadlamudi. His research interests include high voltage engineering, renewable energy systems and hybrid electric vehicles. He has published/presented around 75 research papers in national and international Journals and conferences and granted with two US patents.

1 Introduction

Fuel cell vehicles (FCVs) have the potential to significantly reduce our dependence on foreign oil and lower harmful emissions that cause climate change. FCVs run on hydrogen gas rather than gasoline and emit no harmful tailpipe emissions. These vehicles are in the early stages of development, and several challenges must be overcome before these vehicles will be competitive with conventional vehicles. However, the potential benefits of this technology are substantial.

The heart of the FCV, the fuel cell is a single step energy conversion device which converts the chemical energy directly into electricity obviating the step of chemical combustion used in a typical process of heat extraction from the fuel (Buie et al., 2006). It is a direct single step energy conversion device and is therefore associated with high electrical efficiency. Water and heat are the byproducts of the fuel cell along with electricity when pure hydrogen is used as a fuel and therefore it is clean source of energy. The characteristic features of the fuel cell are high efficiency, zero/low pollutant emission and fuel flexibility. These three features make the fuel cell an extremely desirable option for future power generation.

A proton exchange membrane (PEM) fuel cell consists of three layers, viz., anode, cathode and electrolyte. Hydrogen is made to flow through anode and oxygen traverses through cathode. While hydrogen traverses through anode, it gets reduced to protons and electrons at anode catalyst layer which is made of platinum and supported on carbon back bone. PEM allows only protons to pass through it while electrons would not be allowed as it has affinity towards protons and is phobic towards electrons. Electrons are forced to go through the external circuit to reach cathode thereby completing the circuit and generating DC electricity. A carbon cloth gas diffusion layer (GDL), placed over the catalyst layer, is used to diffuse the reactants uniformly over the PEM. Protons reach the other side of PEM through a process named Grottus mechanism. All the three components, viz., protons through PEM, electrons from external circuit and oxygen through cathode GDL meet at cathode catalyst layer. This chemical reaction gives out water and heat.

Cells that take oxygen by passive means through natural convection are known as air-breathing fuel cells (ABFCs). The performance of the ABFC gets affected by the type of the cathode used. Ribbed (planar) and ducted (channel) designs are the two commonly used cathode designs (Babu et al., 2016). The performance of ABFC is less compared to PEM fuel cell due to mass transportation losses and water management.

Hydrogen is humidified to enhance the ionic conductivity of PEM. While protons travel through membrane, they drag water molecules through the membrane. This phenomenon is referred to as electro-osmotic drag (Chen and Zhao, 2005; Larminie and Dicks, 2000). Under certain operating conditions, water concentration levels on cathode side are higher than anode side owing to water produced during electrochemical reaction as well as electro-osmotic drag. This creates a favourable condition for the water to move from cathode to anode. This phenomenon is referred to as back diffusion (Larminie and Dicks, 2000). At low current densities, back diffusion dominates electro-osmosis while at high current densities, electro-osmosis dominates back diffusion and the anode will tend to dry out, even if the cathode is well hydrated (Sridhar, 2002; Colinart et al., 2009).

The protonic conductivity of Nafion membrane depends mainly on the water content. The protons migrate through hydrated membrane by dissociating the sulphonic acid bond (Stumper et al., 2005). The conductivity of a fully hydrated Nafion membrane is 300 times more than that of a dry one (Zawodzinski et al., 1995). In addition, lack of water affects the performance of fuel cell as the number of active reaction sites of the three-phase boundary decreases (Hickner et al., 2006). The drying out of the membrane at the anode side is more prevalent as electro-osmotic drag dominates at high current densities and also due to the electrochemical water production at the cathode side (Zhou et al., 2006). Finally, severe dehydration conditions lead to the degradation of the membrane due to the occurrence of delamination and pinholes in about 100 s (Knights et al., 2004; Okada, 1999).

On the contrary, the water accumulated in the flow channels and/or GDLs leads to the blockage of the pores on the carbon papers and ultimately impedes the diffusion of the reactant gases to the active reaction sites of the three-phase boundary causes flooding (Stumper et al., 2005). The cell flooding proceeds in two stages: first, slight decline in the cell voltage due to the accumulation of water in the flow channels and second, rapid fall

in the cell voltage after several minutes due to the blockage of the pores in the GDLs, hindering the flow of reactant gases to the active reaction sites of the three-phase boundaries (Mason et al., 2013).

Flooding takes place at both anode and cathode but it is more crucial at cathode owing to the production of electrochemical water due to oxygen reduction reaction (Barbir et al., 2005; Natarajan and Nguyen, 2005; Meng and Wang, 2005). Due to the production of water in the catalyst layer, flooding takes place initially in the catalyst layer followed by GDLs and flow field channels. On the other hand, when the humidity of the reactant gases is high and also when the cell temperature is low, flooding is expected to occur in the flow field channels alone without flooding actually taking place in the catalyst layer and GDLs (Spernjak et al., 2007).

The short-term effects of flooding are reversible, whereas exposure to excess water for long periods of time causes degradation of the material used for the fabrication of MEA (Yousfi-Steiner et al., 2008). As an upshot, to avert the degradation and to assure high performance, a subtle equilibrium has to be found between dehydration and excess water flooding. In order to avert severe dehydration the humidity of the air must be maintained at over 80% and must be under 100% to prevent excess water stagnation in the electrodes/flow channels (Barbir, 2005).

Many diagnostic tools have been proposed to detect the operating states of the fuel cell: A fault tree was built to distinguish between the operating states of a fuel cell by observing their causes and symptoms (Yousfi-Steiner et al., 2008). A neural network based black-box tool was developed to predict the operating states of a fuel cell using difference between the predicted and calculated values of cell voltage and pressure drop as a deciding factor (Steiner et al., 2010; Escobet et al., 2009). An analytical method is proposed to detect the operating states of a fuel cell by using median voltage of the stack as a decisive element (Escobet et al., 2009). In another method a sensing electrode is used to detect the operating states of a fuel cell (Herrera et al., 2009).

In this paper, a novel diagnosing technique for an air-breathing fuel cell (ABFC) is proposed to identify dehydration, normal and flooding states using easily measurable parameters like cell temperature, voltage and current. Preliminarily, by considering iR drop as distinguishing parameter, dehydration and normal/flooding states are distinguished. Comprehensive understanding of normal, flooding and dehydration states is presented through experimental investigations.

2 Experimental setup

The membrane electrode assembly (MEA) is fabricated with an active area of 5 cm^2, with a Pt/C (40%) catalyst loading of 1 mg/cm^2 on both the electrodes. Nafion–117 is used as an electrolyte membrane in this study. The single cell assembly is shown in Figure 1.

The experiments are conducted using Model 850e compact fuel cell test facility as shown in Figure 2 to obtain the V-I characteristic of the fuel cell.

Figure 1 Assembled fuel cell (see online version for colours)

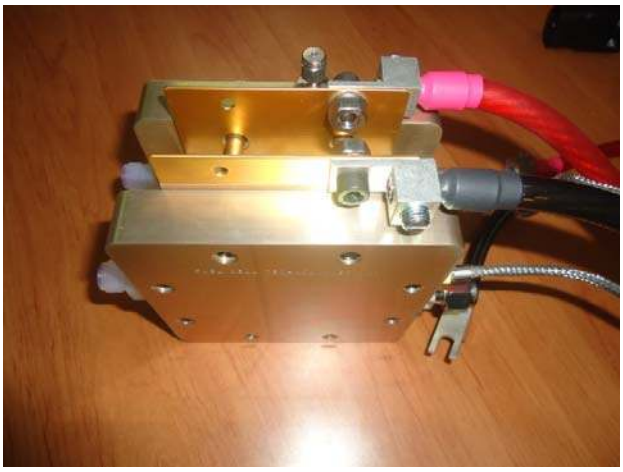

Figure 2 Fuel cell test station (see online version for colours)

3 Results and discussion

The operating characteristics of an ABFC at a cell temperature of 30°C, anode saturation temperature of 40°C and hydrogen flow rate of 0.05 LPM are shown in Figure 3. It is observed that open circuit voltage and limiting current density are 0.98 mA/cm^2 and 110 mA/cm^2 respectively.

3.1 Diagnosis of dehydration, flooding and normal operating condition

The observed cell resistance curves at various cell temperatures and current densities for duration of 1 h are shown in Figure 4.

Figure 3 Operating characteristics of an ABFC (see online version for colours)

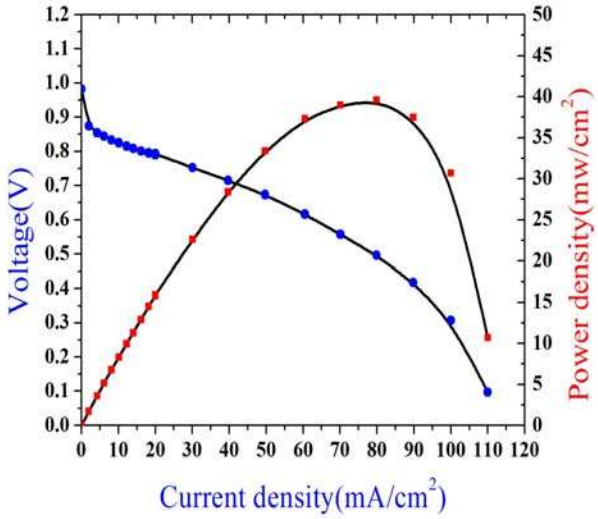

Figure 4 Cell resistance curves for duration of 1 h (see online version for colours)

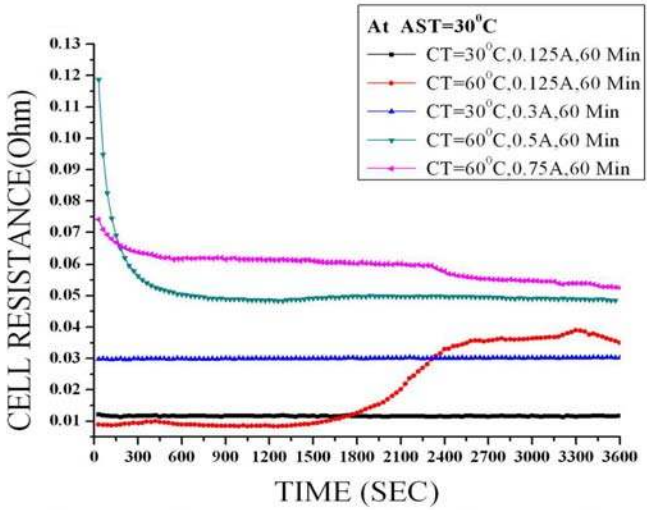

The observed cell voltage curves at various cell temperatures and current densities for duration of 1 h are shown in Figure 5. The observations obtained from cell voltage and cell resistance curves for 1 h duration are tabulated in Table 1. It is observed at a cell temperature (CT) of 60°C, anode saturation temperature (AST) of 30°C and at a current of 0.125 A, the resistance of the cell is increased, clearly indicating dehydration of the cell. Whereas at a CT of 60°C, AST of 30°C and at currents 0.5 A and 0.75 A, the resistance is slightly decreased, clearly indicating flooding in the cell. It is inferred that high temperatures and lower current densities are favourable conditions for dehydration. Also, it is inferred that low temperatures and high current densities as well as high temperatures and medium current densities are favourable conditions for flooding.

Figure 5 Cell voltage curves for duration of 1 h (see online version for colours)

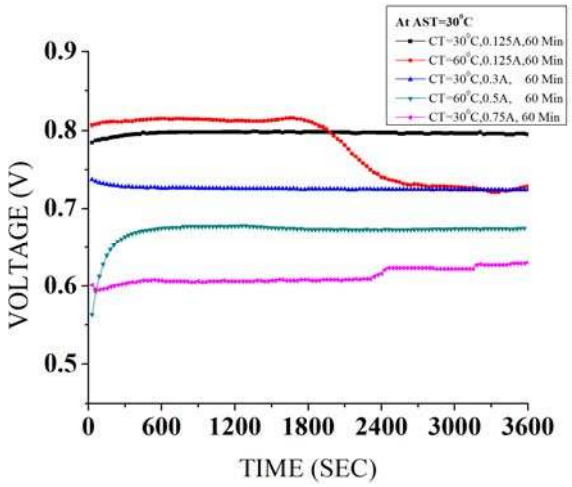

The observed cell resistance curves at various cell temperatures and current densities for duration of 3 h are shown in Figure 6.

Figure 6 Cell resistance curves for duration of 3 h (see online version for colours)

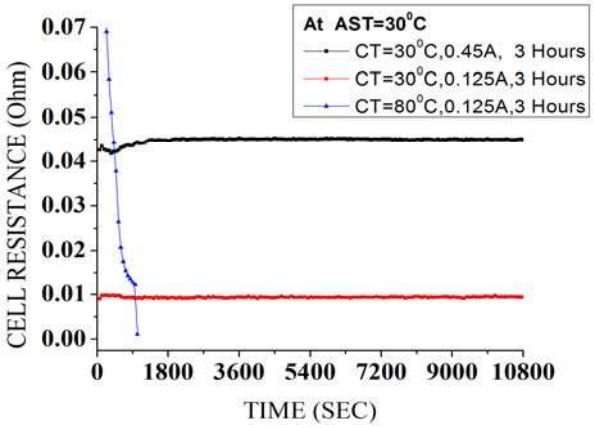

Table 1 Observations for 1 h duration

Cell temperature (°C)	*Anode saturation temperature (°C)*	*Current (A)*	*Inference*
30	30	0.125	Normal operation
60	30	0.125	Dehydration
30	30	0.3	Normal operation
60	30	0.5	Flooding
30	30	0.75	Flooding

The observed cell voltage curves at various cell temperatures and current densities for duration of 3 h are shown in Figure 7.

Figure 7 Cell voltage curves for duration of 3 h (see online version for colours)

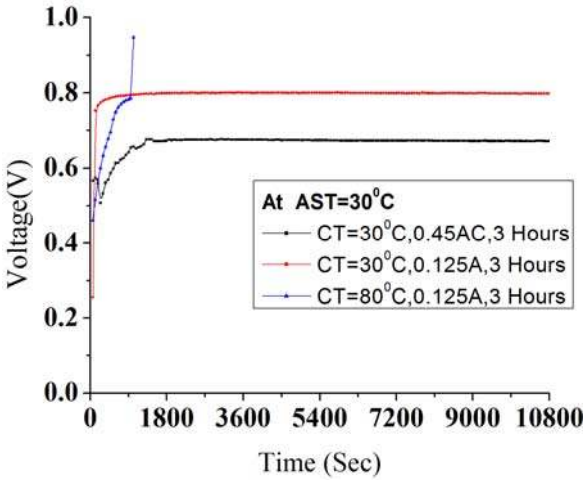

The observations obtained from cell resistance and cell voltage curves for 3 h duration are tabulated in Table 2. It is observed that at a CT of 80°C, AST of 30°C and at a current of 0.125A, the resistance of the cell is increased, clearly indicating dehydration of the cell. Whereas at CT of 30°C, AST of 30°C and at current 0.45A, the resistance is slightly decreased, clearly indicating flooding in the cell. It is inferred that high temperatures and lower current densities are favourable conditions for dehydration. Also, it is inferred that low temperatures and high current densities are favourable conditions for flooding.

Table 2 Observations for 3 h duration

Cell temperature (℃)	*Anode saturation temperature (℃)*	*Current (A)*	*Inference*
30	30	0.45	Flooding
30	30	0.125	Normal operation
80	30	0.125	Dehydration

3.2 Dynamic characteristics

In these dynamic characteristics, to observe the operating states of a fuel cell, a step change in load is applied.

3.2.1 Observed cell resistance curves for low current densities

Figure 8 depicts the dynamic behaviour of the cell resistance when step change in current is applied. The cell resistance is increased from 1875 mΩ to 3250 mΩ as the current stepped up from 0.075 mA/cm^2 to 0.175 mA/cm^2 at a CT of 60°C, AST of 30°C, clearly indicating dehydration of the cell.

Figure 8 Cell resistance curves at low current densities (see online version for colours)

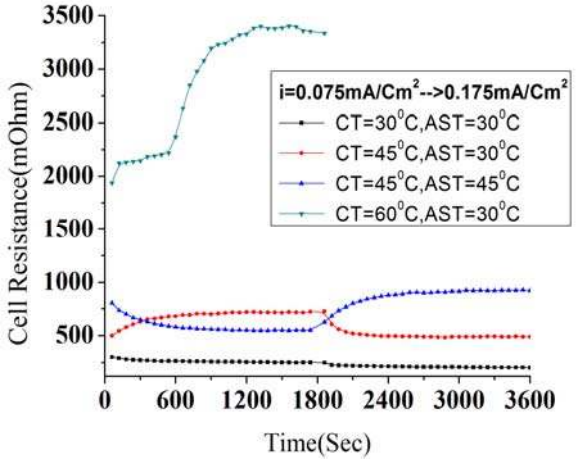

3.2.2 Observed cell voltage curves for low current densities

The dynamic response of the cell voltage when the current is stepped up from 0.075 mA/cm^2 to 0.175 mA/cm^2 at different operating conditions is presented in Figure 9. The cell voltage is reduced to 0.1 V from 0.5 V as the current stepped up from 0.075 mA/cm^2 to 0.175 mA/cm^2 at a CT of 60°C, AST of 30°C, clearly conforming dehydration of the cell. Even though the resistance of the cell is decreased in Figure 7 as the current stepped up from 0.075 mA/cm^2 to 0.175 mA/cm^2 at CT of 45°C, AST of 30°C, the cell voltage in Figure 8 is slightly decreased, clearly indicating flooding in the cell.

Figure 9 Cell voltage curves at low current densities (see online version for colours)

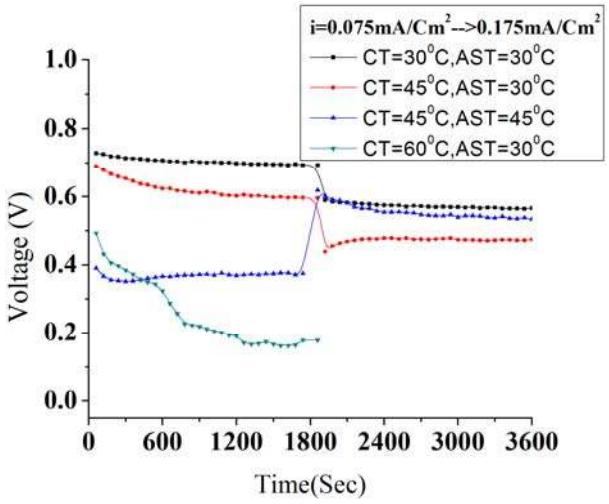

3.2.3 Observed cell resistance curves high current densities

Figure 10 depicts the dynamic behaviour of the cell resistance when the current is stepped up from 0.2 mA/cm^2 to 0.4 mA/cm^2 at different operating conditions. The cell voltage is decreased from 500 mΩ to 1250 mΩ as the current stepped up from 0.2 mA/cm^2 to 0.4 mA/cm^2 at a CT of 60°C, AST of 30°C clearly indicating dehydration of the cell.

Figure 10 Cell resistance curves at high current densities (see online version for colours)

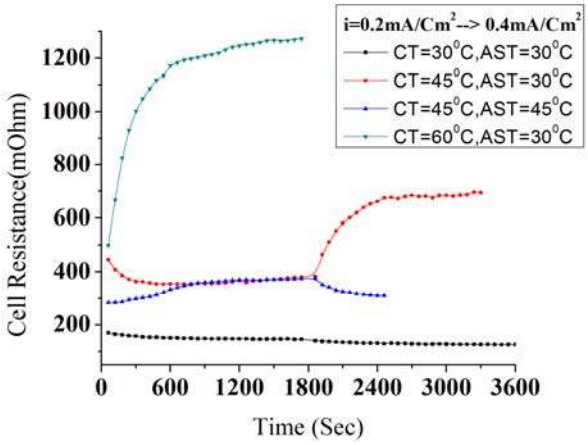

3.2.4 Observed cell voltage curves for high current densities

Figure 11 depicts the dynamic behaviour of the cell voltage when the current is stepped up from 0.2 mA/cm^2 to 0.4 mA/cm^2 at different operating conditions. The cell potential is reduced to 0.1V from 0.5 V as the current stepped up from 0.2 mA/cm^2 to 0.4 mA/cm^2 at a CT of 60°C, AST of 30°C clearly conforming dehydration of the cell.

Figure 11 Cell voltage curves at high current densities (see online version for colours)

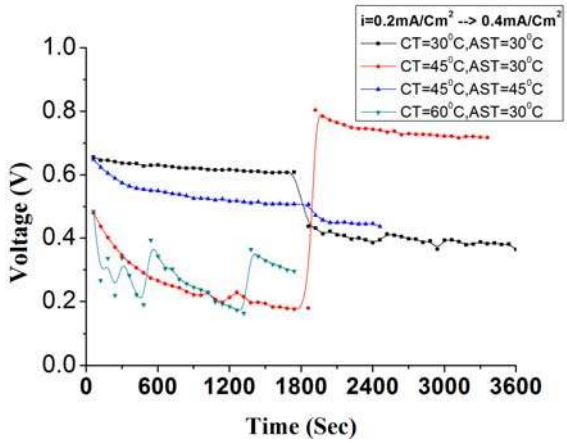

4 Conclusion

This paper addresses the issue of water management in ABFCs by a novel method. Comprehensive understanding of normal, flooding and dehydration states is presented through experimental investigations. Experiments are conducted at various operating conditions to identify dehydration, normal and flooding states using easily measurable parameters like cell temperature, voltage and current. Preliminarily, by considering resistance of the cell as distinguishing parameter dehydration and flooding operating states are distinguished. When the resistance of the cell is in between 120 mΩ and 225 mΩ, flooding is ensured in the cell and the dehydration is ensured when the resistance of the cell is above 225 mΩ.

Acknowledgements

The authors would like to thank the support of the PSGIAS for their kind cooperation during this work.

References

Babu, A.R.V., Kumar, P.M. and Srinivasa Rao, G. (2016) 'Effect of design and operating parameters on the performance of planar and ducted cathode structures of an air-breathing PEM fuel cell', *Arab J. Sci. Eng*., Vol. 41, No. 9, pp.3415–3423, DOI: https://doi.org/10.1007/s13369-015-1890-8.

Barbir, F. (2005) *PEM Fuel Cells: Theory & Practice*, 1st ed., Elsevier Academic Press, California.

Barbir, F., Gorgun, H. and Wang, X. (2005) 'Relationship between pressure drop and cell resistance as a diagnostic tool for PEM fuel cells', *J. Power Sources*, Vol. 141, No. 1, pp.96–101, DOI: https://doi.org/10.1016/j.jpowsour.2004.08.055.

Buie, C., Posner, J.D., Fabian, T., Cha, S., Kim, D., Prinz, F.B., Eaton, J.K. and Santiago, J.G. (2006) 'Water management in proton exchange membrane fuel cells using integrated electroosmotic pumping', *J. Power Sources*, Vol. 161, pp.191–202, DOI: https://doi.org/10.1016/j.jpowsour.2006.03.021.

Chen, R. and Zhao, T.S. (2005) 'Mathematical modeling of a passive-feed DMFC with heat transfer effect', *J. Power Sources*, Vol. 152, pp.122–130, DOI: https://doi.org/10.1016/j.jpowsour.2005.02.088.

Colinart, T., Chenu, A., Didierjean, S., Lottin, O. and Besse, S. (2009) 'Experimental study on water transport coefficient in proton exchange membrane fuel cell', *J. Power Sources*, Vol. 190, No. 2, pp.230–240, DOI: https://doi.org/10.1016/j.jpowsour.2009.01.038.

Escobet, T., Feroldi, D., Lira, S.d., Puig, V., Quevedo, J., Riera, J. and Serra, M. (2009) 'Model-based fault diagnosis in PEM fuel cell systems', *J. Power Sources*, Vol. 192, No. 1, pp.216–223, DOI: https://doi.org/10.1016/j.jpowsour.2008.12.014.

Hickner, M.A., Fujimoto, C.H. and Cornelius, C.J. (2006) 'Transport in sulfonated poly(phenylene)s: Proton conductivity, permeability, and the state of water', *Polymer*, Vol. 47, No. 11, pp.4238–4244, DOI: https://doi.org/10.1016/j.polymer.2006.02.034.

Knights, S.D., Colbow, K.M., St-Pierre, J. and Wilkinson, D.P. (2004) 'Aging mechanisms and lifetime of PEFC and DMFC', *J. Power Sources*, Vol. 127, No. 1, pp.127–134, DOI: https://doi.org/10.1016/j.jpowsour.2003.09.033.

Larminie, J. and Dicks, A. (2000) *Fuel Cell System Explained*, 1st ed., John Wiley & Sons, West Sussex, England.

Mason, T.J., Millichamp, J., Neville, T.P., Shearing, P.R., Simons, S. and Brett, D.J.L. (2013) 'A study of the effect of water management and electrode flooding on the dimensional change of polymer electrolyte fuel cells', *J. Power Sources*, Vol. 242, pp.70-77, DOI: https://doi.org/10.1016/j.jpowsour.2013.05.045.

Meng, H. and Wang, C-Y. (2005) 'Model of two-phase flow and flooding dynamics in polymer electrolyte fuel cells', *J. Electrochem. Soc*., Vol. 152, No. 9, pp.1733–1741, DOI: https://doi.org/10.1149/1.1955007.

Natarajan, D. and Nguyen, T.V. (2005) 'Current distribution in PEM fuel cells. Part 1: Oxygen and fuel flow rate effects', *AIChE, J*., Vol. 51, No. 9, pp.2587–2598, DOI: https://doi.org/10.1002/aic.10545.

O'Rourke, J., Ramani, M. and Arcak, M. (2009) 'In situ detection of anode flooding of a PEM fuel cell', *J. Hydrogen Energy*, Vol. 34, No. 16, pp.6765–6770, DOI: https://doi.org/10.1016/j.ijhydene.2009.06.029.

Okada, T. (1999) 'Theory for water management in membranes for polymer electrolyte fuel cells: Part 1. The effect of impurity ions at the anode side on the membrane performances', *J. Electroanal. Chem*., Vol. 465, No. 1, pp.1–17, DOI: https://doi.org/10.1016/S0022-0728(99)00065-0.

Spernjak, D., Prasad, A.K. and Advani, S.G. (2007) 'Experimental investigation of liquid water formation and transport in a transparent single-serpentine PEM fuel cell', *J. Power Sources*, Vol. 170, No. 2, pp.334–344, DOI: https://doi.org/10.1016/j.jpowsour.2007.04.020.

Sridhar, P. (2002) 'Humidification studies on polymer electrolyte membrane fuel cell', *Fuel and Energy Abst*., Vol. 43, No. 4, p.262, DOI :https://doi.org/10.1016/S0140-6701(02)86296-8.

Steiner, N.Y., Candusso, D., Hissel, D. and Mocoteguy, P. (2010) 'Model-based diagnosis for proton exchange membrane fuel cells', *J. Mathematics and Computers in Simulation*, Vol. 81, pp.158–170, DOI: https://doi.org/10.1016/j.matcom.2010.02.006.

Stumper, J., Löhr, M. and Hamada, S. (2005) 'Diagnostic tools for liquid water in PEM fuel cells', *J. Power Sources*, Vol. 143, pp.150–157, DOI: https://doi.org/10.1016/j.jpowsour.2004.11.036.

Yousfi-Steiner, N., Mocotéguy, Ph., Candusso, D., Hissel, D., Hernandez, A., Aslanides, A. (2008) 'A review on PEM voltage degradation associated with water management: Impacts, influent factors and characterization', *J. Power Sources*, Vol. 183, No. 1, pp.260–274, DOI: https://doi.org/10.1016/j.jpowsour.2008.04.037.

Zawodzinski, T.A., Davey, J., Jestel, R., Lopez, C., Valerio, J. and Gottesfeld, S. (1995) 'The water content dependence of electro-osmotic drag in proton-conducting polymer electrolytes', *J. Electrochim. Acta*, Vol. 40, No. 3, pp.297–302, DOI: https://doi.org/10.1016/0013-4686(94)00277-8.

Zhou, B., Huang, W., Zong, Y. and Sobiesiak, A. (2006) 'Water and pressure effects on a single PEM fuel cell', *J. Power Sources*, Vol. 155, No. 2, pp.190–202, DOI: https://doi.org/10.1016/j.jpowsour.2005.04.027.